Electronic Structures and Magnetism of AgCrCh_2 (Ch = S, Se, Te): A Density Functional Theory Study

Helge Rosner[#], Seojin Kim, Yurii Prots, Marcus Schmidt, Jörg Sichelschmidt and Michael Baenitz

Non-oxy delafossites ABCh_2 with a magnetic transition metal on the B site show a plethora of exciting electronic and magnetic properties. Since there is still comparatively little research in this area, we focused on the systematic investigation of the isostructural AgCrCh_2 family with Ch being a member of the chalcogens. In close collaboration with the experiment, we applied density functional calculations to study the influence of chalcogen exchange on the structural, electronic and magnetic properties of the compound family. As results, we find a strong and systematic dependence of the electronic gap size, the band widths and splittings due to different covalency and spin-orbit couplings in the compound series. Our study extends to the investigation of spin-polarized surface states with possible spintronic functionality.

Covalently bonded two dimensional structures are frequently found with the triangular motif realized by a simple planar hexagonal lattice, in particular, but also by more complex geometries such as a honeycomb lattice. Due to the anisotropic hybridization of electronic states, anisotropic metallic conductivity and magnetic couplings devolve through a specific bonding situation shaped by the underlying crystal structure. In contrast to the oxygen based delafossites which usually form in the centrosymmetric space group R-3m, the related non-oxy compounds often do not exhibit inversion symmetry (see Figure 1).

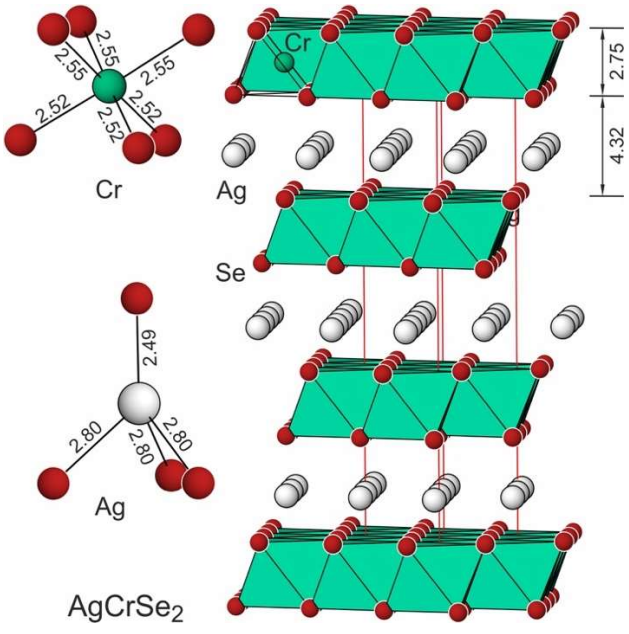

Fig. 1: Crystal structure of the non-centrosymmetric $AgCrSe_2$ (space group R3m). The $CrSe_2$ layers are formed by almost regular, face sharing $CrSe_6$ octahedra (green), whereas the $AgSe_4$ tetrahedra are strongly irregular. The numbers provide the thickness of the layers and the bond lengths in Ångström.

As a consequence of additionally broken symmetries, these systems show rather exotic properties in their transport and magnetic properties, like (for Ch = Se) an anomalous Hall effect in presence of anisotropic cycloidal magnetic order. While experimental studies on the thermodynamic, magnetic and transport properties are the subject of other highlight reports (see **PQM_01_Baenitz**, **PQM_07_Zhang**), we report here in detail on the electronic structure of AgCrCh_2 and the respective changes when varying the chalcogen atom Ch (Ch = S → Se → Te). For our investigation, we apply the density function (DFT) all electron full potential code FPLO [1], including spin-orbit-coupling (SOC) and a mean field approximation to treat strong Coulomb repulsion (LDA+U).

Figure 2 shows the calculated total and partial densities of states (DOS) for $AgCrSe_2$ for different scenarios. Without taking into account the local spin polarization at the Cr site, we find a metallic solution with a high Cr DOS at the Fermi level E_F due to the half-filled Cr 3d t_{2g} bands in agreement with a formally three valent Cr. In agreement with the almost cubic crystal field, the unoccupied e_g states are well separated by about 2 eV from the t_{2g} bands. The rather high DOS at E_F suggests a magnetic instability. Experimentally, a complex magnetic order with a cycloidal planar magnetic order in the Cr-Se layers and antiferromagnetic order between the layers (k = (0.037, 0.037, 3/2)) has been observed (see **PQM_01_Baenitz** and references therein). Since the in-plane order is very close to ferromagnetic order (FM) and the coupling between the layers is small, we use the FM state as a good approximation for our study. The Cr related bands near E_F are rather narrow, thus for a spin polarized calculation the large exchange splitting in the Cr 3d shell opens a very narrow gap of about 15 meV at E_F.

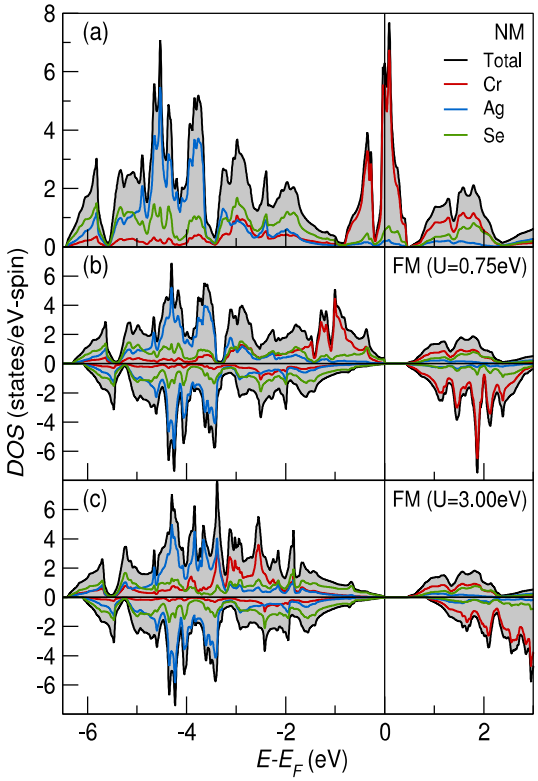

Fig. 2: Total and partial electronic densities of states of $AgCrSe_2$. (a) Nonmagnetic metallic solution with dominating Cr 3d states at the Fermi energy E_F, (b) Ferromagnetic insulating state including spin-orbit coupling for U = 0.75 eV and (c) U = 3 eV. [2]

This is in qualitative agreement with experiments which find the compound to be a self-doped semiconductor with a small charge carrier density and magnetic moments on the Cr site [2, 4]. However, for intermetallic compounds with magnetic 3*d* transition elements, strong Coulomb correlations that are not well described in standard DFT calculations may play an important role. To investigate the relevance of strong correlations for the low energy electronic structure of $AgCrSe_2$, the comparison of the DFT calculations applying a varying Hubbard *U* with spectroscopic measurements is a suitable procedure.

Figure 3a shows XAS measurements of the Cr $L_{2,3}$ edge. Its shape is characteristic of a dominant Cr^{3+} configuration. In agreement with the DFT results, a Cr $3d^3$ electronic configuration would thus be expected to first order, with a half-filled t_{2g} shell. However, in contrast to Figure 2a, the measurements of the valence DOS (Figure 3b) indicate only a weak step at the Fermi level, with the majority of the occupied DOS located at higher binding energy.

The photoemission measurements were performed with photon energies spanning the Cr L3 x-ray absorption edge (Figure 3b). They observe a marked increase in the spectral weight of the peak in the DOS centered at ~1.5 eV binding energy when the photon energy is tuned into resonance with the corresponding Cr 2*p*–3*d* transition. This indicates that this feature has a dominantly Cr-derived character, whose spectral weight becomes enhanced "on-resonance." From the difference of the photoemission spectra measured on and just below the resonance energy, an experimental measure of the Cr partial DOS can be extracted (Figure 2c). This confirms that there is negligible Cr DOS at the Fermi level. As the measurements are performed well above the magnetic ordering temperature of $AgCrSe_2$, this provides initial evidence for the persistence of a well-defined local moment above TN.

To quantify the electronic correlations, we compare the experimental Cr partial DOS with that calculated from DFT (Figure 3c and Figure 2). A clear disagreement is found with the nonmagnetic DFT calculations, where a large Cr DOS is obtained at the Fermi level, unlike that obtained experimentally. We thus compare with our magnetic LDA+*U* calculations, where the strength of the Hubbard-*U* parameter is varied. Taking a value of *U* = 3 eV, typical for Cr-based oxides, we find that the Cr DOS is peaked at too high a binding energy as compared to the experiment. Moreover, rather than having a single dominant peak as for the *U* = 3 eV calculations, the experimental partial DOS has a double-peak structure with spectral weight distributed

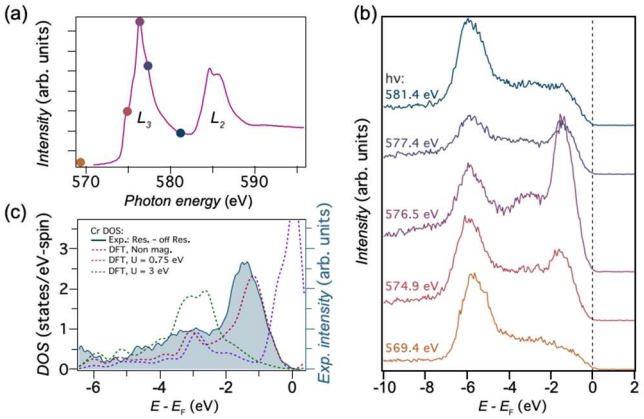

Fig. 3: (a) X-ray absorption spectroscopy at the Cr $L_{2,3}$ edge, indicating a dominant Cr^{3+} valence. (b) Angle-integrated resonant photoemission measurements of the valence band electronic structure, measured at the photon energies marked by the points in (a) which span across the L3 edge. (c) The Cr partial density of states extracted experimentally as the difference of the on- and off-resonant PES spectra (hv = 576.5 eV and 569.4 eV, respectively; solid blue line with shading). The dashed lines show the corresponding Cr partial DOS as determined by nonmagnetic DFT, and by LDA+U calculations for U = 0.75 eV and 3 eV, respectively. [2]

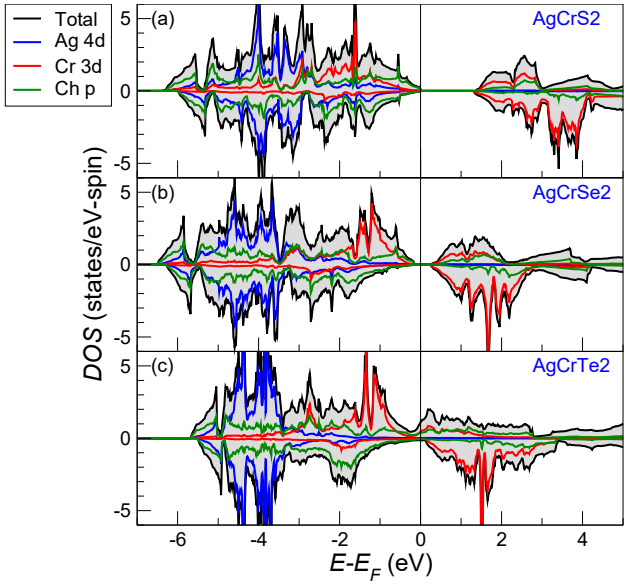

Fig. 4: Total and partial electronic densities of states of ferromagnetic (a) $AgCrS_2$ (U = 3eV), (b) $AgCrSe_2$ (U = 0.75 eV) and (c) $AgCrTe_2$ (U = 0).

throughout the valence band. Indeed, much better agreement with both the locations and overall shape of the experimental DOS is obtained for calculations using a low U value of 0.75 eV. This points to a much more weakly correlated state as compared to, e.g. $PdCrO_2$, where the Cr-derived states in $AgCrSe_2$ become more strongly hybridized with the ligand states.

The large difference in correlation between *Ch* = O or *Ch* = Se for the chalcogen site draws our interest to the influence of chalcogen substitution (*Ch* = S → Se → Te) on the electronic structure. In Figure 4, the DOS of these materials is arranged according to the position of the chalcogen element in the periodic table. At first glance, as expected for the isostructural and isovalent compounds, their DOS's look similar regarding the overall shape and the energy region of the constituents. In general, the width of the valence band decreases moving from S to Te. This points to an increasing covalency between Cr and the chalcogenide and in turn, to an increasing delocalization of the hybridized Cr 3*d* states and a decreased size of correlation. To describe the experimentally observed electronic gap in $AgCrS_2$, a rather large Hubbard U of 3eV is required compared to the 0.75 eV for $AgCrSe_2$ matching the PES results (see Figure 3c). For *Ch* = Te, the size of correlations should further decrease. Since U values up to 2 eV did not open an electronic gap here, we expect the compound to be a metallic magnet. Unfortunately, up to now all attempts to synthesize the system failed, so that a comparison of this prediction with the experiment is not possible at present.

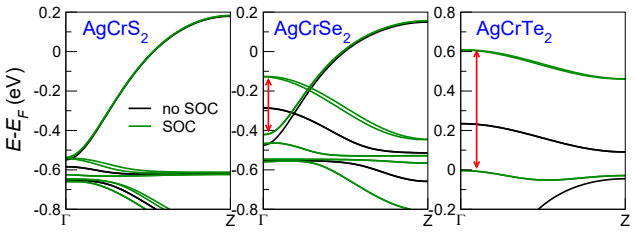

Fig. 5: Band structures without (black) and without (green) SOC. The size of the split due to SOC (marked by red arrows) is negligible (about 30 meV at Γ) for $AgCrS_2$, very significant for $AgCrSe_2$ (about 300 meV at Γ) and even larger for $AgCrTe_2$ (about 600 meV at Γ).

In addition to the strongly varying correlation with respect to chalcogen substitution, also the influence of SOC to the states near E_F changes dramatically. This is demonstrated in Figure 5. Since for all three compounds the bands near E_F are dominated by the p states of the chalcogen ligand (see Figure 4), the SOC for these bands scales with its atomic mass and comes close to the atomic value in the respective chalcogenide p states. The large SOC splitting of these band in $AgCrSe_2$ is a prerequisite for the large, unconventional anomalous Hall effect observed in the experiment [4] and likely also responsible for its complex magnetic structure. In this regard, a successful synthesis of the likely metallic $AgCrTe_2$ would be even more interesting.

Stimulated by the successful description of the bulk electronic structure by DFT, we also studied the surface electronic structure of $AgCrSe_2$ [3]. Through comparison of microscopic-area angle-resolved photoemission with our first-principles calculations, we unveil the striking role of the SOC for a surface hole gas, unlocked by both bulk and surface inversion symmetry breaking. In contrast to the small Fermi pockets expected for a self-doped semiconductor, the ARPES measurements reveal two bands crossing E_F with large k_F values (see Figure 6a, b). The associated carrier density in comparison to the Hall measurements [4] appears far too high to derive from the bulk states. Combined with the strong spatial variation in the measured electronic structure observed here, we thus instead attribute these metallic states as the result of a significant additional hole doping at the $CrSe_2$-terminated surface. Consistent with this, photon energy-dependent ARPES measurements (Figure 6d) indicate that these states are non-dispersive with the out-of-plane momentum across multiple Brillouin zones in k_z. DFT supercell calculations of the surface electronic structure of a $CrSe_2$-terminated slab confirm this assignment (Figure 6c). We find a complex multiband electronic structure throughout the valence bands.

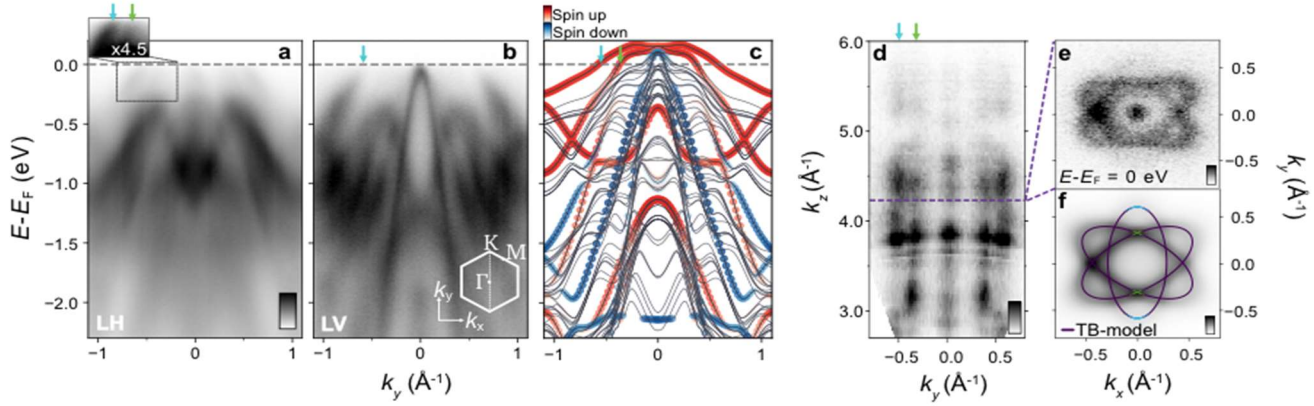

Fig. 6: Electronic structure of the $CrSe_2$-terminated surface. ***(a)***, ***(b)*** *ARPES data from the $CrSe_2$-terminated surface measured along $\Gamma - K$ using hv = 75 eV and a linear horizontal (LH) and b linear vertical (LV) polarized light both measured at a temperature of $T \approx 18$ K below the magnetic transition of $T_N = 32$ K. Two bands can be observed crossing the Fermi level, indicated by the blue and green arrows. The inset in (a) shows the region indicated with enhanced contrast.* ***(c)*** *DFT calculations of a $CrSe_2$-terminated supercell, projected onto the spin-up and spin-down character of the top $CrSe_2$ layer.* ***(d)*** *Photon energy-dependent ARPES measurements (hv = 20–140 eV, LH polarized light, $T \approx 18$ K), allowing probing the momentum distribution curve at the Fermi level over multiple Brillouin zones in k_z.* ***(e)*** *Measured Fermi surface (LH polarized light, $T \approx 8$ K) in the k_x–k_y plane, at the k_z value indicated by the dashed line in* ***(d)***, *and* ***(f)*** *corresponding three-band minimal tight-binding model. [3]*

Of core importance here, however, are the near-E_F states, which we show projected onto the surface $CrSe_2$ layer with spin-up and spin-down characters. From this, we can identify the Fermi surfaces observed experimentally as arising exclusively from the spin-up carriers. Although spin-down states are seen to cross the Fermi level in the calculations, the top of the dispersive hole band visible in Figure 6b is in reality located just below the Fermi level. This discrepancy likely arises due to the slight off-stoichiometry inherent to the slab geometry of a material with polar surfaces. Experimentally, the location of this band just below the Fermi level establishes the surface hole gas here as a half-metal, comprised of just one species of spin-polarized carriers. Excitingly, the spin-majority states are located close by in energy, and so tuning of the Fermi level, for example using the field-effect, could be used to deliberately yield carriers of opposite spin orientation, leading to a tunable spin polarization of the surface layer. Thus, more general, achieving this type of control would allow for gaining electrical control of spintronic functionality in materials hosting similar spin-polarized surface electron gases.

External Cooperation Partners

G.R. Siemann, P. D. C. King (University of St Andrews, United Kingdom); J. Zhu, A.M. Cook, MPI PKS Dresden); L. Smejkal (J. Gutenberg University Mainz).

References

[1] *Full-potential nonorthogonal local-orbital minimum-basis band-structure scheme, K. Koepernik and H. Eschrig, Phys. Rev. B.* ***59*** *(1999) 1743, https://doi.org/10.1103/PhysRevB.59.1743*

[2]* *Planar triangular S =3/2 magnet $AgCrSe_2$: Magnetic frustration, short range correlations, and field-tuned anisotropic cycloidal magnetic order, M. Baenitz, M. M. Piva, S. Luther, J. Sichelschmidt, K. M. Ranjith, H. Dawczak-Debicki, M. O. Ajeesh, S.-J. Kim, G. Siemann, C. Bigi, P. Manuel, D. Khalyavin, D. A. Sokolov, P. Mokhtari, H. Zhang, H. Yasuoka, P. D. C. King, G. Vinai, V. Polewczyk, P. Torelli, J. Wosnitza, U. Burkhardt, B. Schmidt, H. Rosner, S. Wirth, H. Kühne, M. Nicklas, M. Schmidt, Phys. Rev. B.* ***104*** *(2021) 134410, https://doi.org/10.1103/PhysRevB.104.134410*

[3]* *Spin-orbit coupled spin-polarised hole gas at the $CrSe_2$-terminated surface of $AgCrSe_2$, G. R. Siemann, S. J. Kim, E. A. Morales, P. A. E. Murgatroyd, A. Zivanovic, B. Edwards, Marković, F. Mazzola, L. Trzaska, O. J. Clark, C. Bigi, H. Zhang, B. Achinuq, Th. Hesjedal, M. D. Watson, T. K. Kim, P. Bencok, G. van der Laan, C. M. Polley, M. Leandersson, H. Fedderwitz, K. Ali, B.Thiagarajan , M. Schmidt , M. Baenitz, H. Rosner, P. D. C. King, NPJ Quantum Materials* ***8*** *(2023) 61, https://doi.org/10.1038/s41535-023-00593-4*

[4]* *Observation of the Anomalous Hall Effect in a Layered Polar Semiconductor, S. Kim, J. Zhu, M. M. Piva, M. Schmidt, D. Fartab, A. P. Mackenzie, M. Baenitz, M. Nicklas, H. Rosner, A. M. Cook, R. González-Hernández, L. Šmejkal, H. Zhang, Adv. Sci.* ***11*** *(2024) 2307306, https://doi.org/10.1002/advs.202307306*

[#] helge.rosner@cpfs.mpg.de